Supporting Information

Zahn et al. 10.1073/pnas.1320486111

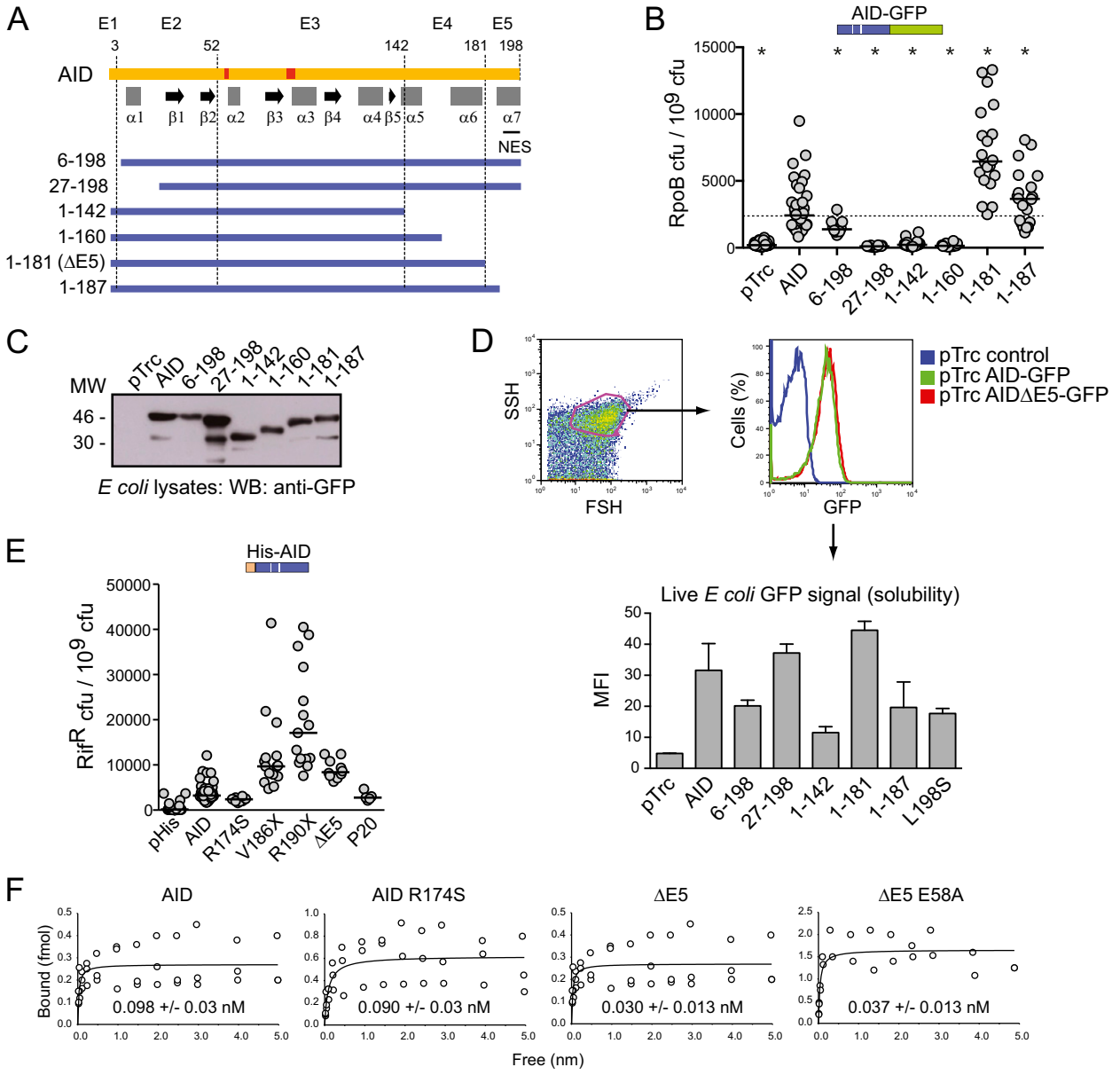

Fig. S1. Exon 5 (E5) is the only domain of activation-induced deaminase (AID) dispensable for enzymatic activity, and it is not required for DNA binding (related to Figs. 1 and 2). (*A*) Schemes of the serially truncated AID variants that were fused to the N terminus of GFP are shown below the AID scheme. Predicted secondary structure and the regions encoded by each *AICDA* exon (E), delimited by dotted lines with the final amino acid position noted, are indicated. NES, nuclear export signal. (*B*) *Escherichia coli* fluctuation assay of *rpoB* mutation frequency. Each symbol indicates the Rif^R cfu in an independent culture expressing AID-GFP variants. pTrc, empty vector control. Data from two to four independent experiments for each variant are compiled, with median values indicated by horizontal lines and significant differences compared with AID (*P* values by Kruskal–Wallis test with Dunnet multiple test comparison; $\alpha <$ 0.05). (*C*) Relative expression of each AID-GFP variant protein in total extracts of induced *E. coli* cultures determined by Western blot (WB). MW, molecular weight markers. (*D*) Relative expression of each AID-GFP variant determined by flow cytometry in live *E. coli* cultures. The gating strategy and GFP signal for representative cultures are shown. SSC-H, side scatter; FSC-H, forward scatter. Mean + SD of the mean fluorescent intensity (MFI) of GFP in three to five induced cultures is plotted. This measurement provides an estimation of the relative expression of soluble protein for each AID variant, because precipitation of the fusion protein would inactivate GFP (1). (*E*) The actual *rpoB* mutation frequencies of the *E. coli* fluctuation assays that are presented as normalized to AID in Fig. 2*A* are plotted as in *A*. pHis, empty vector control. (*F*) DNA binding capacity of AID variants was determined by EMSA and quantified. The results of three experiments are plotted with the fitted average curve and derived mean ± SD. K_d values.

1. Delker RK, Zhou Y, Strikoudis A, Stebbins CE, Papavasiliou FN (2013) Solubility-based genetic screen identifies RING finger protein 126 as an E3 ligase for activation-induced cytidine deaminase. *Proc Natl Acad Sci USA* 110(3):1029–1034.

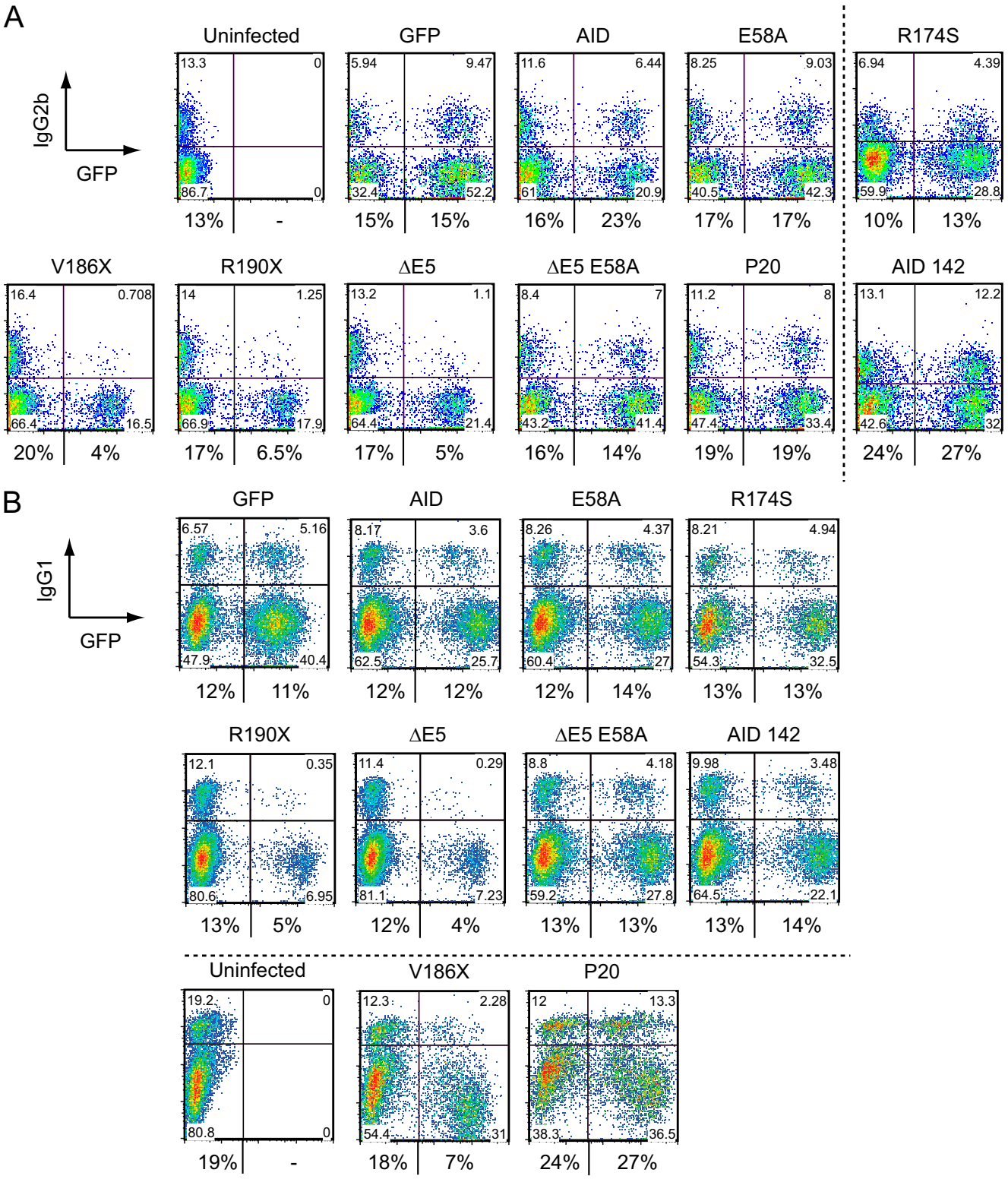

Fig. S2. Representative flow cytometry profiles for class switch recombination (CSR) dominant-negative assays (related to Fig. 1). (*A*) IgG2b CSR assays in WT (*Aicda*$^{+/+}$) B cells retrovirally transduced with the indicated AID variants-ires-GFP vectors. (*B*) IgG1 CSR assays in *Aicda*$^{+/-}$ B cells as in *A*. Plots coming from different experiments are separated by dotted lines. When staining and gating are different, selected controls are presented for comparison. The frequency of each gate is indicated. The proportion of switched cells in GFP^{-} (untransduced) and GFP^{+} (transduced) B cells was calculated and is indicated below the corresponding region.

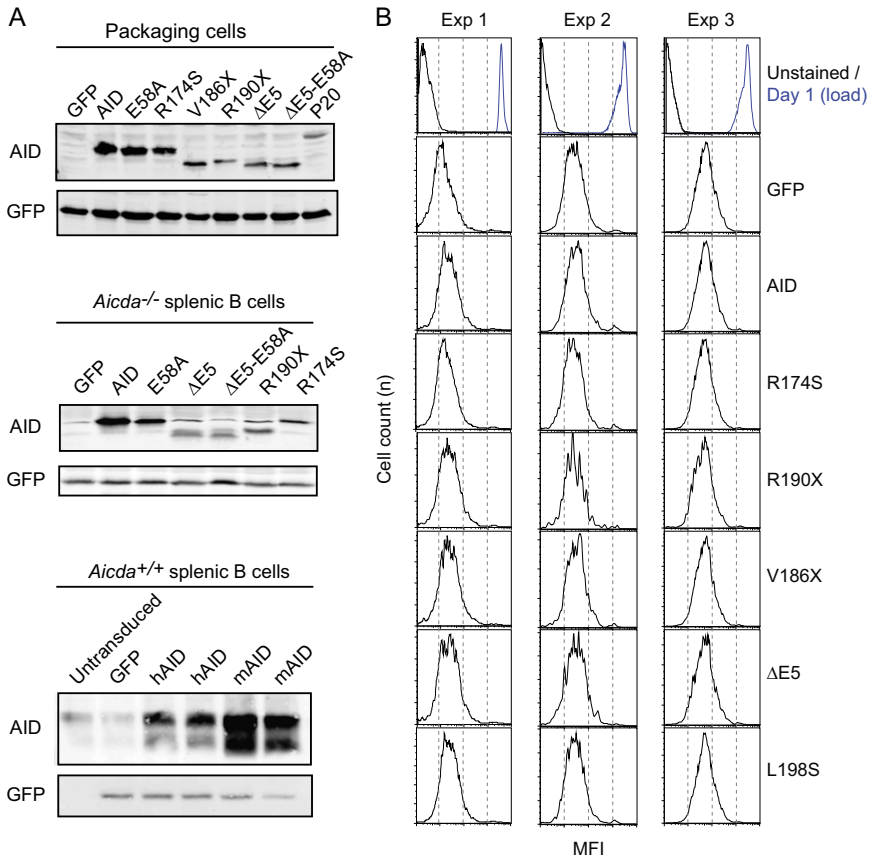

Fig. S3. Relative protein expression levels and effect on cell proliferation of AID variants (related to Fig. 1). (*A*) Comparative expression levels of AID variants in transfected retrovirus packaging cells (*Top*) and retrovirally transduced *Aicda*$^{-/-}$ (*Middle*) and *Aicda*$^{+/+}$ (*Bottom*) primary B cells. The blots in *Top* and *Middle* were probed using a mixture of mAbs 52–1 and 39–1 specific for the N terminus of human AID. Note that these mAbs recognize a weak unspecific band in B cells of the same mobility of AID (also visible in DT40 cells in Fig. 2*D* and Fig. S7*B*). *Bottom* was probed using a rabbit polyclonal antiserum raised against the C-terminal 14 residues of mouse AID (described in ref. 1), which also recognizes human AID. Note that human and mouse AID differ in two positions over the immunizing peptide (mouse EVDDLRDAFR**M**LG**F** vs. human EVDDLRDAFR**T**LG**L**), and therefore, this antiserum reacts less with human than mouse AID. *Bottom* shows human and mouse AID transduced in parallel into B cells from two WT mice using the same vector to show this difference in recognition. Blots were quantified using the Odyssey software (Li-COR), and transduced AID signal was normalized to GFP. Our data indicate an average of ~10- to 12-fold overexpression of transduced WT mouse AID vs. endogenous AID. The AID variants would be expressed proportionally to their relative expression levels, which is shown in *Top* and *Middle*. (*B*) Cell proliferation of WT primary B cells expressing retrovirally delivered AID- or variant-ires-GFP. Flow cytometry histograms showing the dilution of the cell proliferation dye eFluor670 in GFP^{+} cells at 96 h [experiments 1 and 2 (Exps. 1 and 2)] or 72 h (Exp. 3) poststimulation. Row 1 in each experiment shows representative signals of cells immediately after eFluor670 loading (blue profile) and unstained (black profile) as a reference.

1. Chaudhuri J, et al. (2003) Transcription-targeted DNA deamination by the AID antibody diversification enzyme. *Nature* 422(6933):726–730.

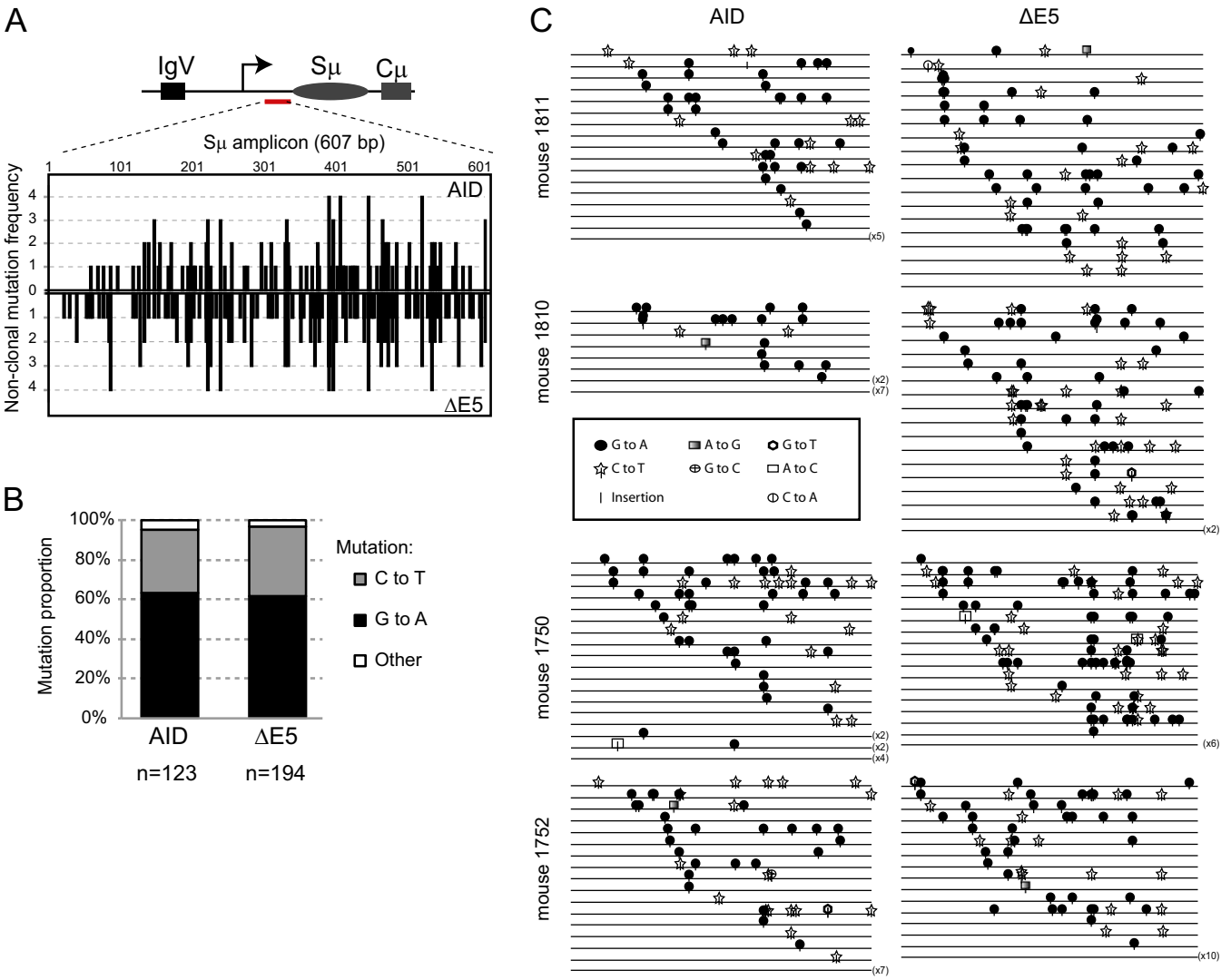

Fig. S4. ΔE5 targets and deaminates the Ig Sμ region with similar quality to AID (related to Fig. 2). (*A*) Distribution of deamination at the indicated Sμ region (628-bp fragment, nucleotides 177959–178587 of NG_005838.1) in *Aicda*$^{-/-}$ *Ung*$^{-/-}$ B cells retrovirally complemented with AID or ΔE5. The plot shows the frequency of independent mutations scored at each position compiled from data obtained from four mice. Identical mutations at the same position were only counted one time among the sequences obtained for each individual mouse. (*B*) Proportion of mutation type as scored on the top strand of the Sμ calculated from the data in *A*. The number of independent mutations analyzed is noted below each bar. The similar proportion of mutations in AID and ΔE5 indicates no difference in their strand preference. (*C*) Schematics of the whole set of sequences obtained from each mouse analyzed in *A*.

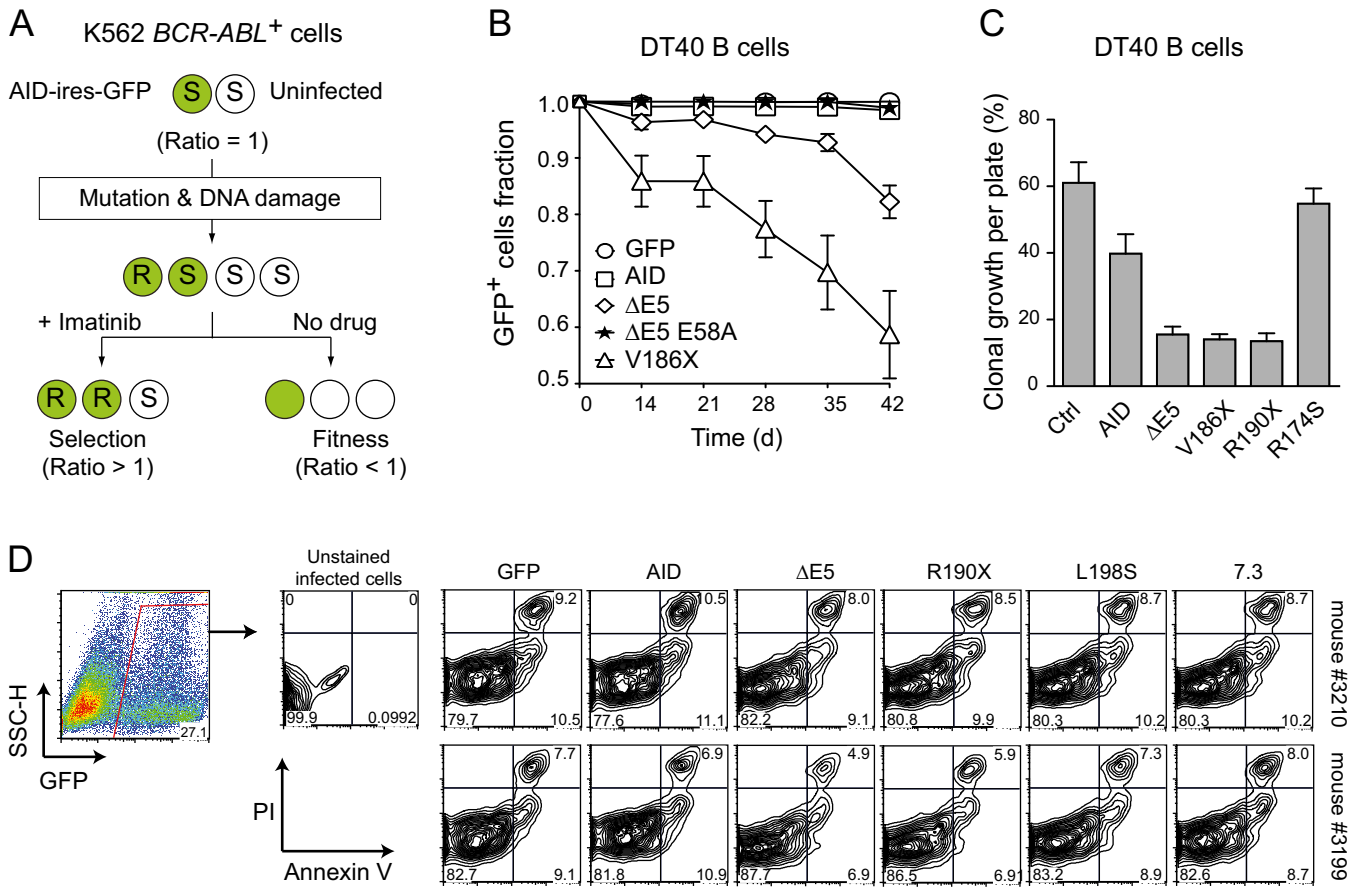

Fig. S5. AID variants with truncated E5 hinder B-cell expansion but do not increase apoptosis (related to Fig. 3). (*A*) Schematics of the assays performed in K562 BCR-ABL$^+$ chronic myelogenous leukemia cells. K562 cells originally sensitive (S) to imatinib were transduced with AID-ires-GFP retroviral vectors and mixed at a 1:1 ratio with untransduced parental cells. AID variants mutate the *BCR-ABL*, and some of the mutations render BCR-ABL kinase resistant to the imatinib inhibitor. GFP signal is periodically monitored by flow cytometry. When grown in the presence of imatinib as the selection agent, an increased ratio of GFP$^+$ (transduced) to GFP$^-$ (untransduced) cells indicates the acquisition of imatinib resistance (R) through AID-dependent mutations at *BCR-ABL*. However, growing the cells without any selection reveals the relative effect of each AID variant on cell fitness. (*B*) Expression stability of the indicated AID variants transduced into DT40 B-cell lines. The expression of each variant is linked through an ires sequence to GFP expression that was monitored by flow cytometry over time after infection in the absence of any selection. (*C*) Clonal growth capacity of sorted *Aicda*$^{-/-}$ DT40 B cells complemented with the indicated AID variants was determined by single cell deposition in 96-well plates. Bars indicate mean + SD of the proportion of wells with viable clones 2 wk after sorting for three plates per construct. Ctrl, control. (*D*) Apoptosis was measured in retrovirally complemented *Aicda*$^{-/-}$ B cells 24 h after infection by Annexin V and propidium iodide (PI) staining. SSC-H, side scatter. One representative of at least two experiments performed with B cells from two mice for each construct are shown.

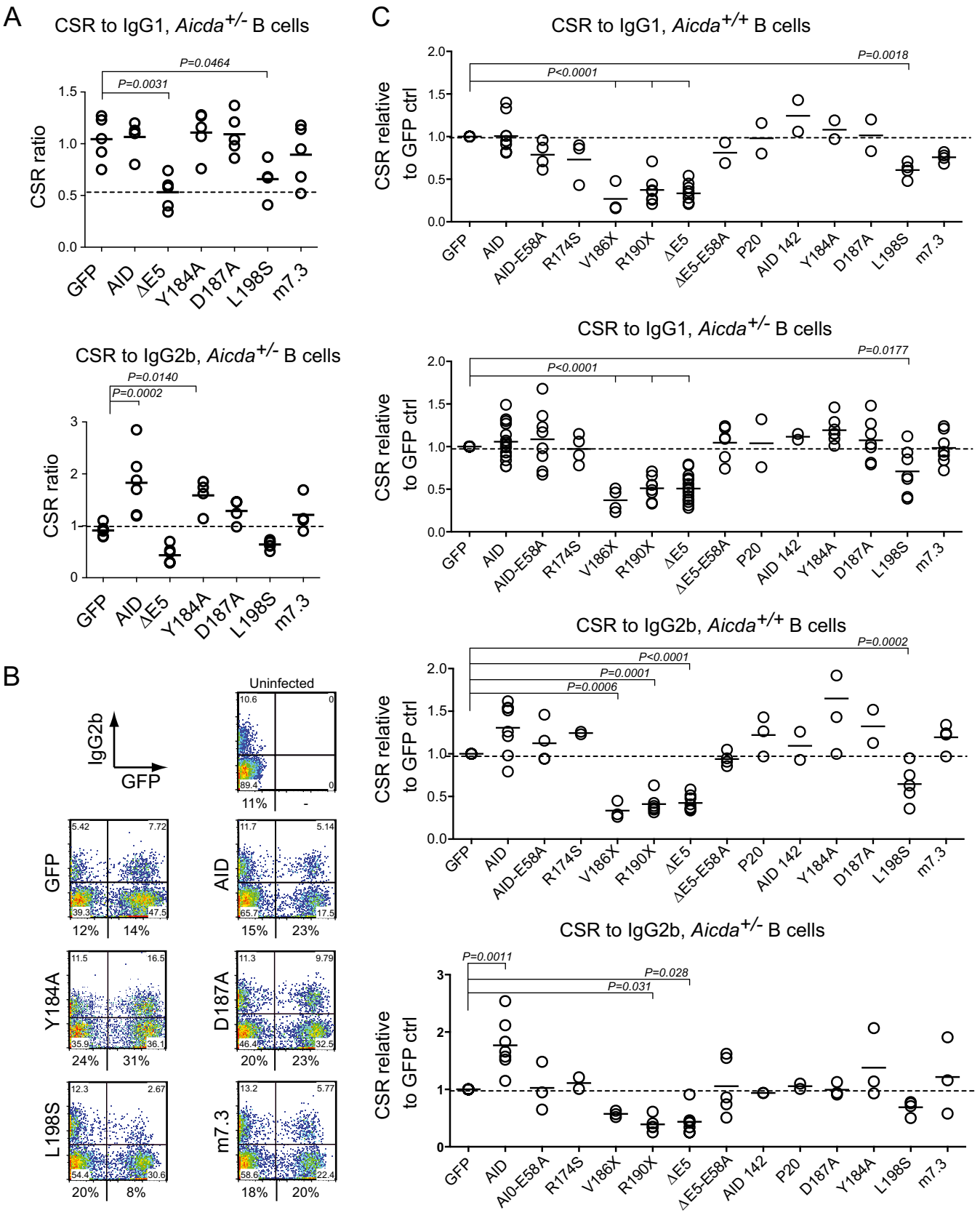

Fig. S6. Dominant-negative behavior of artificial AID point mutants and alternative calculation for the dominant-negative effect (related to Figs. 1 and 4). (*A*) Compiled CSR ratios for IgG1 and IgG2b in *Aicda*$^{+/-}$ B cells transduced with the indicated AID variants. Each symbol is the ratio between the proportion of switched cells in the infected (GFP^{+}; expressing the indicated AID variant) and uninfected (GFP^{-}) fractions of B cells from an individual mouse. A ratio of one is marked by a dotted line. Means are indicated by horizontal bars. Significant *P* values from one-way ANOVA with Dunnet multiple comparisons test are

Legend continued on following page

indicated. (*B*) Representative flow cytometry data of dominant-negative assays performed for IgG2b CSR in WT B cells. (*C*) The effect on CSR was analyzed by normalizing the proportion of switched cells on the infected subpopulation (GFP^+) to their corresponding mock-infected control (expressing only GFP) in each experiment. All experiments from Figs. 1 and 4 are pooled in the graphs, and statistically significant differences compared with the GFP control by ANOVA with Dunnet posttest are indicated.

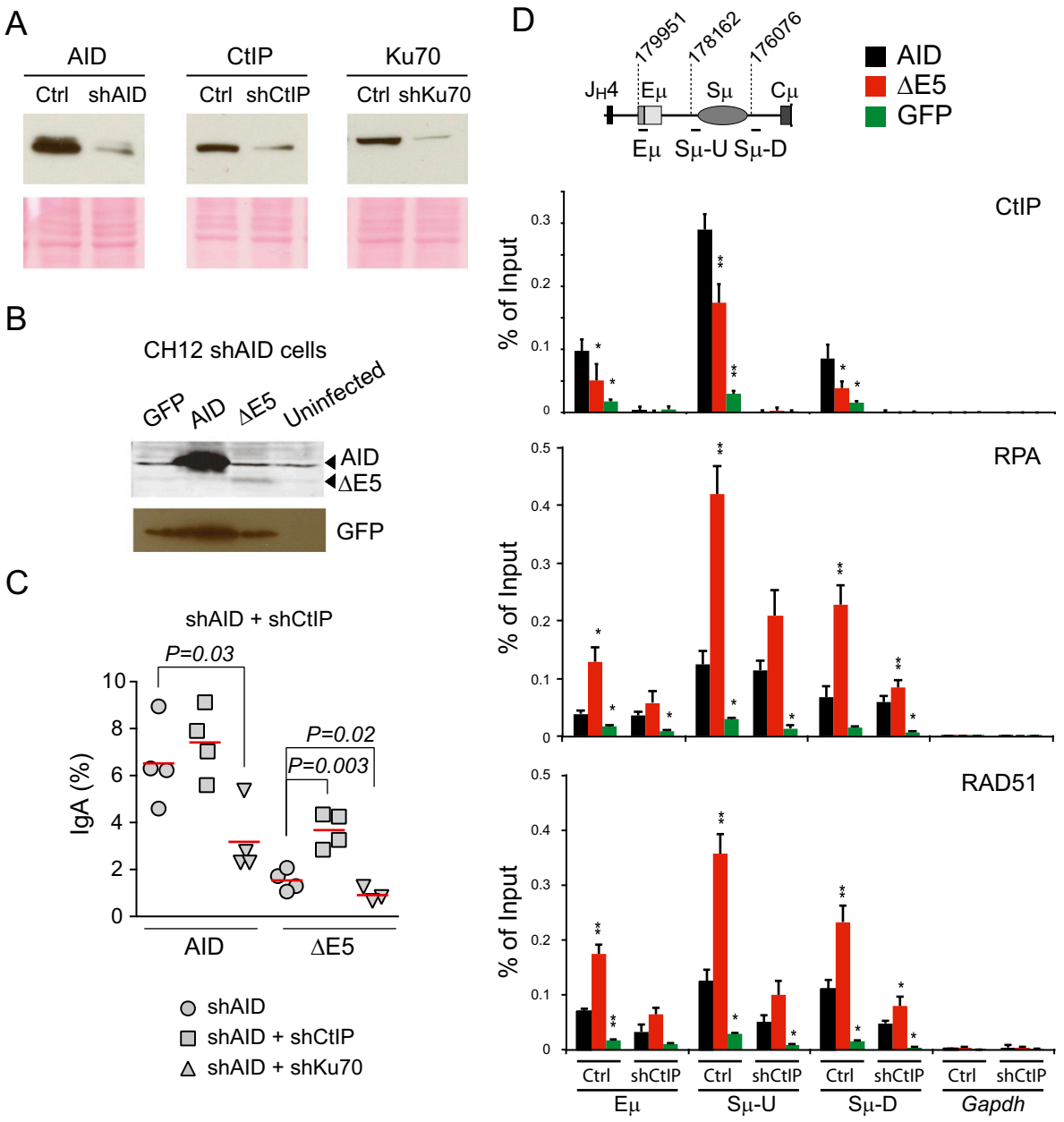

Fig. S7. CtIP depletion in CH12 cells rescues CSR by ΔE5 (related to Fig. 6). (*A*) Western blotting indicating AID, CtIP, and Ku70 protein levels in CH12 cells transduced with retroviruses encoding shRNAs specific for each of those factors after neomycin (shAID) or puromycin (shCtIP and shKu70) selection. AID was probed using polyclonal rabbit antiserum against mouse C terminus. (*B*) Relative expression levels of shRNA-resistant human AID and ΔE5 in complemented CH12 shAID cells were analyzed by Western blot using mAbs 52–1 and 39–1. (*C*) Absolute CSR efficiency data for the experiments presented as normalized in Fig. 6*D*. (*D*) Real-time PCR ChIP assays for CtBP-interacting protein (CtIP), replication protein A (RPA), and the homologous recombination factor RAD51 occupancy at the indicated amplicons in the *Igh* of CH12 cells that were depleted from AID (Ctrl) or AID and CtIP (shCtIP) and complemented with empty vector (GFP), AID, or ΔE5. *Gapdh* region was used as control. Means + SDs of three biological replicates for each variant and condition are plotted. Significant differences compared with AID in each amplicon by ANOVA with Dunnet posttest are indicated (**$P < 0.01$; *$P < 0.05$).

Table S1. Description and summary of the activities of the AID mutants included in this work

Name	Origin	Structure description	*RpoB* mutation *E. coli*	*IgV* SHM DT40	In vitro CSR B cells	γH2AX foci HeLa	CSR dominant negative	Source
AID		WT human AID	+++	+++	+++	–	No	1
AID-E58A	Artificial	Full-length, Asp58 > Ala	–	–	–	–	No	2
R174S	AR HIGM2	Full-length, Arg174 > Ser	+/–	–	–	–	No	3
V186X	AD HIGM2	Truncated form, residues 1–185	++++++	++++++	+/–	+	Yes	4
R190X	AD HIGM2	Truncated form, residues 1–189	++++++	++++++	+/–	+	Yes	5
ΔE5	Artificial	Truncated form, residues 1–181	++++++	++++++	+/–	+	Yes	2
ΔE5-E58A	Artificial	Truncated form, residues 1–181, Asp58 > Ala	–	–	–	–	No	This work
142	Artificial	Truncated form, residues 1–142	–	–	–	–	No	This work
P20	AR HIGM2	Insertion, Leu181 Pro182 34 residues (VTKPSTQFRRLSGPTDPQPRFEAIHSICFSLSLR)	+/–	ND	–	–	No	6
Y184A	Artificial	Full-length, Tyr184 > Ala	++++	+++	+++	–	No	This work
D187A	Artificial	Full-length, Asp187 > Ala	++	+++	+++	–	No	2
m7,3	Artificial	Full-length, Lys10 > Glu, Thr82 > Ile, Glu156 > Gly	++++++	++++++	+++	–	No	7
L198S	Artificial	Full-length, Leu198 > Ser	++++++	++++++	+/–	+	Yes	2

AD, autosomal dominant; AR, autosomal recessive; HIGM2, hyper-IgM immunodeficiency syndrome; *IgV*, Ig variable exon; ND, not done; SHM, somatic hypermutation.

1. Muramatsu M, et al. (1999) Specific expression of activation-induced cytidine deaminase (AID), a novel member of the RNA-editing deaminase family in germinal center B cells. *J Biol Chem* 274(26):18470–18476.
2. Patenaude A-M, et al. (2009) Active nuclear import and cytoplasmic retention of activation-induced deaminase. *Nat Struct Mol Biol* 16(5):517–527.
3. Quartier P, et al. (2004) Clinical, immunologic and genetic analysis of 29 patients with autosomal recessive hyper-IgM syndrome due to Activation-Induced Cytidine Deaminase deficiency. *Clin Immunol* 110(1):22–29.
4. Durandy AH, Taubenheim N, Péron S, Fischer A (2007) Pathophysiology of B-cell intrinsic immunoglobulin class switch recombination deficiencies. *Adv Immunol* 94:275–306.
5. Imai K, et al. (2005) Analysis of class switch recombination and somatic hypermutation in patients affected with autosomal dominant hyper-IgM syndrome type 2. *Clin Immunol* 115(3): 277–285.
6. Ta V-T, et al. (2003) AID mutant analyses indicate requirement for class-switch-specific cofactors. *Nat Immunol* 4(9):843–848.
7. Wang M, Yang Z, Rada C, Neuberger MS (2009) AID upmutants isolated using a high-throughput screen highlight the immunity/cancer balance limiting DNA deaminase activity. *Nat Struct Mol Biol* 16(7):769–776.